Predictions for a Distributed Parameter Model Describing the Hepatic Processing of 2,3,7,8-TCDD*

H. T. Banks†, C. J. Musante‡, and J. K. Raye
Center for Research in Scientific Computation, and
Department of Mathematics
North Carolina State University
Raleigh, NC 27695-8205

November 1, 1998, Revised February 15, 1999

Abstract

A distributed parameter model describing spatially-dependent hepatic processing of the chemical compound 2,3,7,8-tetrachlorodibenzo-*p*-dioxin (TCDD or dioxin) has previously been reported [1]. The mathematical system consists of coupled nonlinear partial and ordinary differential equations with delays. In this paper we investigate the qualitative behavior of the system over a six-hour time period following a subcutaneous injection. A brief summary of the model is also given.

Keywords and phrases: Distributed parameter models, pharmacokinetic models, 2,3,7,8-tetrachlorodibenzo-*p*-dioxin, liver transport models, delay equations.

1 Introduction

Numerous physiologically-based pharmacokinetic (PBPK) models have been developed to describe the uptake and elimination of the environmental toxin 2,3,7,8-tetrachlorodibenzo-*p*-dioxin (for example, see [2]–[6]). While most PBPK models assume well-mixed compartments, recent work [1, 6, 7] has focused on the development of advanced techniques to account for spatially-dependent tissue responses.

In rodents, TCDD has been shown to bind to two hepatic proteins: the aryl hydrocarbon (Ah) receptor [8] and an inducible protein, cytochrome P4501A2 (CYP1A2) [9, 10]. Following administration of TCDD, binding to the Ah receptor results in a dose-dependent induction of CYP1A2 [9, 10]; therefore, this protein is present at both a basal (non-induced) and induced level in the presence of TCDD. The liver response to dioxin is not homogeneous, resulting in preferential localization around centrilobular regions at low doses [6]. Lumped parameter PBPK models, which assume a uniform concentration of the toxin throughout the liver, cannot account for this known heterogeneity in cellular response.

A partial differential equation model to describe the spatially-dependent hepatic processing of TCDD has been proposed [1, 11] and is briefly summarized in Section 2. In Section 3 the numerical scheme used in solving the resultant system of equations is given. Our preliminary

*This research was supported in part by the Air Force Office of Scientific Research (AFOSR) under Grants F-49620-95-1-0236, F-49620-98-1-0180, F-49620-95-1-0375, and F-49620-93-1-0355. The research of CJM and JKR was funded by US Department of Education Graduate Assistance in Areas of National Need (GAANN) Fellowships under Grants P200A50075 and P200A70707, respectively. CJM also received support from the 1997 AFOSR Graduate Summer Research Program and the Armstrong Laboratory.

†Author to whom correspondence should be addressed.

‡Current address: U.S. Environmental Protection Agency, National Health and Environmental Effects Research Laboratory, Experimental Toxicology Division, Mail Drop 74, Research Triangle Park, NC 27711.

computational results on the qualitative behavior of the system are discussed in Section 4. In particular, we examined the behavior of the system on the time interval from zero to six hours, prior to TCDD-induced CYP1A2 synthesis. We also studied the dependence of the solution on two important model parameters, the dispersion number, $\mathcal{D}_N$, and a circulatory delay, τ_c. Finally, in Section 5 we discuss future research directions.

2 The TCDD Model

A mathematical model (1) has been developed [1, 11] to describe pharmacokinetic and pharmacodynamic properties of TCDD. A convection-dispersion equation (1a), based on the work of Roberts and Rowland [12], characterizes the transport of blood elements in the liver sinusoidal (blood) region. Throughout this discussion, the dimensionless spatial variable x takes on values in the range $[0, 1]$; $x = 0$ corresponds to the liver inlet, while $x = 1$ corresponds to the outlet. Uptake of dioxin into the hepatic cells, called hepatocytes, is assumed to occur by passive diffusion. The model includes the dynamics of TCDD-binding with two intracellular hepatic proteins, the Ah receptor (1c)-(1d) and an inducible microsomal protein, CYP1A2 (1e)-(1f). The induction mechanism is described in terms of the fractional occupancy of the Ah receptor at a previous time, $t - \tau_r$, to account for the many intracellular processes which must occur before an increase in CYP1A2 concentration is realized. Elimination in the liver (by metabolism and biliary clearance) is assumed to be a first order process.

A well-mixed, combined venous/arterial blood compartment (1g), which includes a loss due to the uptake and elimination of TCDD in the rest of the body, completes the system. A circulatory lag, τ_c, accounts for the time delay in transport of blood elements from the exit of the liver to the venous measurement location.

The mathematical system under consideration is as follows:

$$(V_B + V_D \frac{f_{u_B}}{f_{u_D}}) \frac{\partial C_B}{\partial t} = Q\mathcal{D}_N \frac{\partial^2 C_B}{\partial x^2} - Q\frac{\partial C_B}{\partial x} + P(C_{u_H} - f_{u_B} C_B), \tag{1a}$$

$$\begin{aligned} \frac{\partial C_{u_H}}{\partial t} &= \frac{P f_{u_B}}{V_H} C_B - (\frac{P}{V_H} + k_3) C_{u_H} - g_{Ah}(C_{u_H}, C_{Ah}) \\ &\quad + k_{-1} C_{Ah-T} - g_{Pr}(C_{u_H}, C_{Pr}) + k_{-2} C_{Pr-T}, \end{aligned} \tag{1b}$$

$$\frac{\partial C_{Ah-T}}{\partial t} = g_{Ah}(C_{u_H}, C_{Ah}) - k_{-1} C_{Ah-T}, \tag{1c}$$

$$\frac{\partial C_{Ah}}{\partial t} = k_{-1} C_{Ah-T} - g_{Ah}(C_{u_H}, C_{Ah}) - k_{d(Ah)} C_{Ah} + k_{s(Ah)}, \tag{1d}$$

$$\frac{\partial C_{Pr-T}}{\partial t} = g_{Pr}(C_{u_H}, C_{Pr}) - k_{-2} C_{Pr-T}, \tag{1e}$$

$$\begin{aligned} \frac{\partial C_{Pr}}{\partial t} &= k_{-2} C_{Pr-T} - g_{Pr}(C_{u_H}, C_{Pr}) - k_{d(Pr)} C_{Pr} + k_{s(Pr)} \\ &\quad + I_{Pr} \frac{C_{Ah-T}(t - \tau_r, x)}{C_{Ah}(t - \tau_r, x) + C_{Ah-T}(t - \tau_r, x)}, \end{aligned} \tag{1f}$$

$$\frac{dC_a}{dt}(t) = \frac{Q_a}{V_a}(C_B(t - \tau_c, 1) - C_a(t)) + I(t) - k_e C_a(t), \tag{1g}$$

$$\begin{aligned} &C(s, x) = \Phi(x), \quad s \in [-\tau_r, 0], \\ &C_B(t, 0) = C_a(t), \\ &QC_B(t, 1) - Q\mathcal{D}_N \tfrac{\partial C_B}{\partial x}(t, 1) = Aq_2(t), \end{aligned} \tag{1h}$$

where $C = [C_B, C_{u_H}, C_{Ah-T}, C_{Ah}, C_{Pr-T}, C_{Pr}, C_a]^T$. In Eqn. (1h), Φ and Aq_2 are assumed known.

We note that g_{Ah} and g_{Pr} are saturating nonlinearities modified from the usual product

terms,

$$\tilde{g}_{Ah}(y,z) = k_{+1}yz, \tag{2}$$
$$\tilde{g}_{Pr}(y,z) = k_{+2}yz, \qquad \text{for } y,z \in \mathbb{R}, \tag{3}$$

arising from the *law of mass action* in chemical kinetics. Specifically, we assume that within a certain range of concentrations the system behaves according to the nonlinearities prescribed by (2) and (3) but eventually saturates; i.e., due to the availability of binding species, we assume the rates of formation of Ah-TCDD complex and CYP1A2-TCDD complex are bounded.

The mathematical model (1) consists of a nonlinear system of partial differential equations with delays and questions of well-posedness are of interest. Detailed general theories of existence, uniqueness, and continuous dependence for certain nonlinear parabolic systems (including the TCDD model) are given in [11, 13]. Furthermore, a general result for related least-squares parameter estimation problems is given in [14]. These results were obtained using a weak or variational formulation of the problem and are based on ideas from the works of Banks *et al.* [15]-[16] for nonlinear hyperbolic systems.

The summary given above, while brief, is included to provide the reader with a general understanding of the complex dynamics of the system under investigation. The reader is referred to the aforementioned works [1, 11, 13, 14] for complete discussions.

3 Numerical Methods

In this section we present an overview of the numerical methods used in our simulations. All coefficient matrices, functions, vectors, etc. are as described in [11].

Our numerical scheme is based on a weak formulation [13] of the problem given in Eqn. (1). To obtain the weak form, we multiplied the i^{th} equation by a function ψ_i in a "suitable" class of test functions and then integrated in space in the first six equations, followed by integration by parts in Eqn. (1a) only.

For ease of notation, we define

$$y = [C_B, C_{u_H}, C_{Ah-T}, C_{Ah}, C_{Pr-T}, C_{Pr}, C_a]^T = [y_1, \ldots, y_7]^T.$$

3.1 Finite Element Formulation

Let $0 = x_0 < x_1 < \ldots < x_N = 1$ be a uniform partition of the interval $[0,1]$ into N subintervals of length $h = 1/N$. We take as basis elements the piecewise linear continuous functions, ϕ_j, $j = 0, \ldots, N$, defined by

$$\phi_j(x) = \begin{cases} \frac{x - x_{j-1}}{h}, & x_{j-1} \le x \le x_j, \\ \frac{x_{j+1} - x}{h}, & x_j \le x \le x_{j+1}, \\ 0, & 0 \le x \le x_{j-1} \text{ or } x_{j+1} \le x \le 1. \end{cases}$$

We define the Galerkin finite element approximations by

$$\begin{aligned} y_1^N(t,x) &= \textstyle\sum_{j=1}^N \alpha_j^1(t)\phi_j(x), \\ y_i^N(t,x) &= \textstyle\sum_{j=0}^N \alpha_j^i(t)\phi_j(x), \end{aligned} \tag{4}$$

for $i = 2, \ldots, 6$, where the basis elements, ϕ_j, are as described above and $y_i^N \approx y_i$.

Next we substitute the finite element approximations (4) into the weak form of the equations. Let $y^N(t) \in \mathbb{R}^{N+5(N+1)+1}$ such that

$$y^N(t) = [\alpha^1(t), \alpha^2(t), \ldots, \alpha^6(t), y_7(t)]^T.$$

The finite dimensional system we obtain, in terms of the time-dependent coefficients of the Galerkin approximations, is given by

$$\mathcal{M}\dot{y}^N(t) = \mathcal{A}y^N(t) + \mathcal{G}_p(y^N(t)) + \mathcal{F}(t) + \mathcal{A}_D y^N(t - \tau_c) + \mathcal{G}_s(y^N(t - \tau_r)), \tag{5}$$

where the matrices $\mathcal{M}$ and $\mathcal{A}$ are elements of $\mathbb{R}^{(N+5(N+1)+1)\times(N+5(N+1)+1)}$ and the vector-valued functions $\mathcal{G}_p$, $\mathcal{F}$, $\mathcal{A}_D$, and $\mathcal{G}_s$ are elements of $\mathbb{R}^{N+5(N+1)+1}$.

The initial condition, y_0^N, for the semi-discrete problem (5) is taken as the L_2 projection of the original initial condition, Φ, onto the finite element space.

3.2 General Algorithm

In these preliminary investigations, we seek solutions on the time interval from zero to six hours. For simplification, we have assumed that no TCDD is present in the system on the interval [-6,0] hours. By making this assumption, we can thereby ignore the induction delay term, $\mathcal{G}_s$, for the purpose of this discussion.

The semi-discrete problem we consider is given by

$$\begin{aligned} \mathcal{M}\dot{y}^N(t) &= \mathcal{A}y^N(t) + \mathcal{G}_p(y^N(t)) + \mathcal{F}(t) + \mathcal{A}_D y^N(t-\tau_c), \\ y^N(s) &= y_0^N(s), \qquad s \in [-\tau_c, 0]. \end{aligned}$$

The entries in the coefficient matrices $\mathcal{M}$ and $\mathcal{A}$, consisting of certain combinations of inner products of basis elements and their derivatives, were calculated analytically rather than through use of a numerical integration scheme. The nonlinear vector function $\mathcal{G}_p$ was treated in a similar manner.

The "method of steps" [17] for ordinary differential equations was used to solve the problem on each delay interval of length τ_c ($\tau_c \ll \tau_r$). The general algorithm is described below:

Algorithm.

- Set T = final time ($T < \tau_r$)
- Form the coefficient matrices $\mathcal{M}$ and $\mathcal{A}$
- Solve the linear system defining the initial condition y_0^N in the finite element space
- Set $t0 = 0$ and $tf = \begin{cases} \tau_c, & \tau_c < T \\ T, & \text{otherwise} \end{cases}$
- do while $t0 < T$
  - Solve on $[t0, tf]$

$$\begin{aligned} \mathcal{M}\dot{y}^N(t) &= \mathcal{A}y^N(t) + \mathcal{G}_p(y^N(t)) + \mathcal{F}(t) + \mathcal{A}_D y_0^N(t-\tau_c) \\ y^N(t0) &= y_0^N(t0). \end{aligned}$$

  - Set $y_0^N(t) = y^N(t)$
  - $t0 = t0 + \tau_c$
    $tf = \begin{cases} t0+\tau_c, & t0+\tau_c < T \\ T, & \text{otherwise} \end{cases}$
- end

In order to evaluate y_0^N, we stored the computed solution throughout the previous delay interval and used an interpolation routine to find the value of the solution at time $t - \tau_c$. In fact, only $(y_0^N)_N$ and $(y_0^N)_{6N+6}$ were stored, as these are the only data required for the linear delay term, $\mathcal{A}_D$.

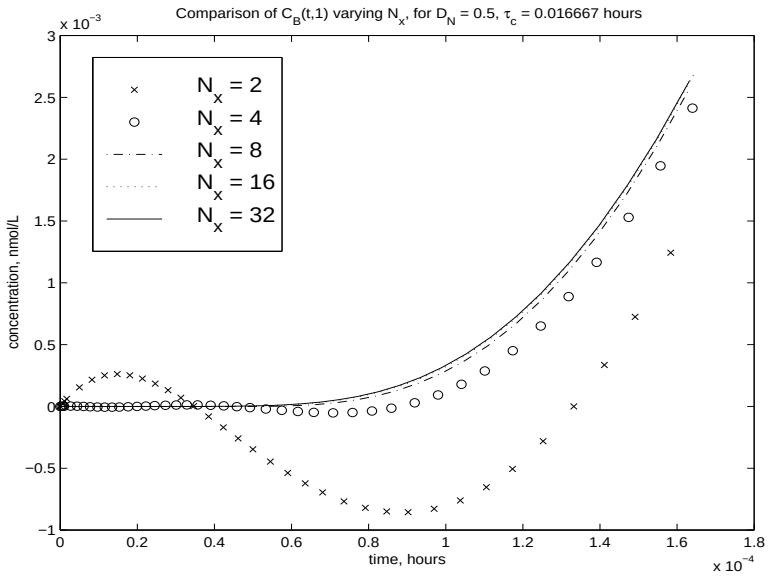

Figure 1: Numerical solution obtained for $C_B(t,1)$ varying the number of basis elements, N_x, with $\mathcal{D}_N = 0.5$. The solutions with $N_x = 16$ and 32 are identical on this scale, indicating convergence of the Galerkin approximations with 16 basis elements.

3.3 Implementation

The computer code was written in MATLAB version 5.1 (The MathWorks, Inc., Natick, MA) and computations were carried out on a Sun Sparc Ultra II workstation and a personal computer with a 180 MHz Intel Pentium Pro processor. The MATLAB routine 'ode15s' [18] was used for time stepping, which is a variable order, variable step method based on numerical differentiation formulas. The relative and absolute error tolerances were set to 1×10^{-6}. Since this is a variable step method, at time t the solution over the previous delay interval had to be interpolated in order to determine the value of the solution at time $t - \tau_c$. MATLAB's interpolation routine 'interp1' was used with the 'spline' option. This method fits the data with cubic splines between data points, so that each segment of the curve fit has at least the same first and second derivatives as the ones adjoining it. The maximum order of the integrator was set to two in order for it to be in the range of accuracy of both the interpolation routine and the finite element approximations.

3.3.1 Convergence of the Numerical Scheme

The theoretical results presented in [11, 14] guarantee convergence of the Galerkin finite element approximation scheme. However, we must determine the number, N, of basis elements to be used in meaningful simulations. We computed solutions over the time span from 0 to 1 hour with fixed $\mathcal{D}_N$ and τ_c, and varied N. Numerical results obtained using a small number of basis elements and t very close to zero exhibited dynamics which were only eventually resolved by decreasing the size of the spatial grid. This behavior is shown in Figure 1 with $\mathcal{D}_N = 0.5$. For values of the dispersion number of interest (0.5–100), we found that increasing $\mathcal{D}_N$ generally resulted in a decrease in the number of basis elements required. For example, convergence was obtained with 16 basis elements for the case $\mathcal{D}_N = 5$ (Figure 2), as compared to just 8 basis elements for $\mathcal{D}_N = 10$ (Figure 3).

Increasing the dispersion number has the effect of smoothing concentration gradients along the cylinder's length [12]; that is, spatial variations in concentrations decrease with increasing $\mathcal{D}_N$, and therefore a less-refined spatial grid is required to capture system dynamics.

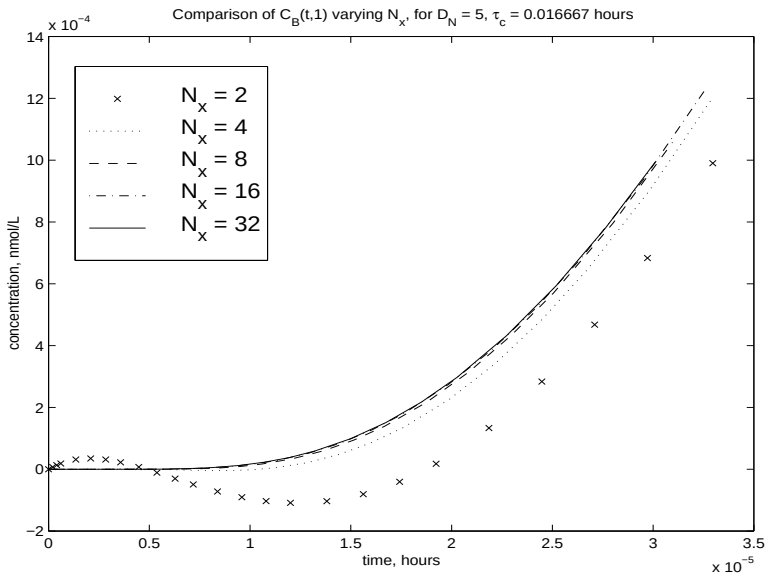

Figure 2: Numerical solution obtained for $C_B(t,1)$ varying the number of basis elements, N_x, with $\mathcal{D}_N = 5$. The solutions with $N_x = 16$ and $N_x = 32$ are identical on this scale, indicating convergence of the Galerkin approximations with 16 basis elements.

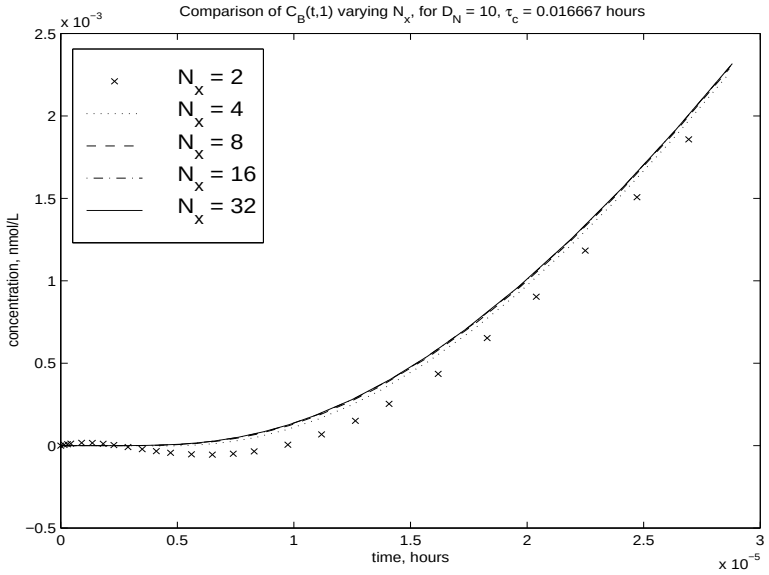

Figure 3: Numerical solution for $C_B(t,1)$ varying the number of basis elements, N_x, with $\mathcal{D}_N = 10$. The solutions with $N_x = 8, 16$, and 32 are identical on this scale, indicating convergence of the Galerkin approximations with 8 basis elements.

4 Model Simulations

4.1 Parameter Estimates, Boundary and Initial Conditions

The majority of parameters used in these simulations were obtained from the literature (see [11]). However, in order to qualitatively estimate the time-dependent exit flux term, $Aq_2(t)$, we implemented a numerical scheme for the TCDD model satisfying a homogeneous Neumann boundary condition, $\frac{\partial C_B}{\partial x}(t,1) = 0$. From a balance of fluxes we have

$$Q(C_B(t,1) - \mathcal{D}_N \frac{\partial C_B}{\partial x}(t,1)) = Aq_2(t), \tag{6}$$

from which we obtained a discrete approximation to Aq_2:

$$Aq_2(t_i) = QC_B(t_i,1).$$

This data was then interpolated and used as an estimate for Aq_2 when simulating model behavior with the Robin boundary condition (6).

All simulations were carried out assuming zero initial conditions for concentrations involving TCDD. Constant values were assumed for the initial levels of the Ah receptor and the induced binding species, CYP1A2. Uptake of TCDD into the arterial/venous blood supply, $I(t)$, was assumed to be from a subcutaneous dose of 300 ng/kg body weight. This was described as a first-order process with rate constant 0.05/hour, as in the work of Anderson *et al.* [5].

The qualitative behavior of the system was investigated while values for the axial dispersion number, $\mathcal{D}_N$, and the circulatory delay, τ_c, were varied, holding all other biological and physiological parameters fixed.

4.2 Predicted Behavior

The system was studied for $\mathcal{D}_N = 50$, $\tau_c = 1$ minute, and $0 \leq t \leq 6$ hours. The most interesting behavior occurs within the first two hours. As the concentration of TCDD in the liver blood increases (Figure 4), free dioxin in the cells is quickly bound to the Ah receptor and CYP1A2. The Ah receptor quickly becomes saturated (Figure 5) due to its low binding capacity. The concentration of the AhR-TCDD complex continues to rise, however, as newly synthesized protein binds any available TCDD. Inactivation of the Ah receptor is modeled as a first-order process (concentration dependent), so that at low concentrations the zero-order process of protein synthesis dominates; that is, there is a net increase in cellular levels of receptor available for binding.

The second dioxin-binding species, CYP1A2, takes longer to become saturated than the Ah receptor because of its higher binding capacity (Figure 6). After roughly two hours, the concentration of free CYP1A2 is essentially depleted, as any newly synthesized protein rapidly binds to free dioxin in the cells. A comparison of unbound TCDD in the liver blood to that in the hepatocytes is given in Figure 7. The binding of TCDD to intracellular proteins causes an initial decrease in the cellular concentration of free dioxin relative to that in the blood. Once the two proteins become saturated, however, the unbound concentration of TCDD in the cells begins to rise, but at no time does the cellular concentration exceed that in the blood. In other words, for this set of model parameters the hepatocytes act as a sink.

4.3 Dependence on the Circulatory Delay

The rate of change of the combined arterial/venous blood compartment is given by the differential equation

$$\frac{dC_a}{dt}(t) = \frac{Q_a}{V_a}(C_B(t-\tau_c,1) - C_a(t)) + I(t) - k_e C_a(t), \tag{7}$$

with initial condition

$$C_a(0) = 0. \tag{8}$$

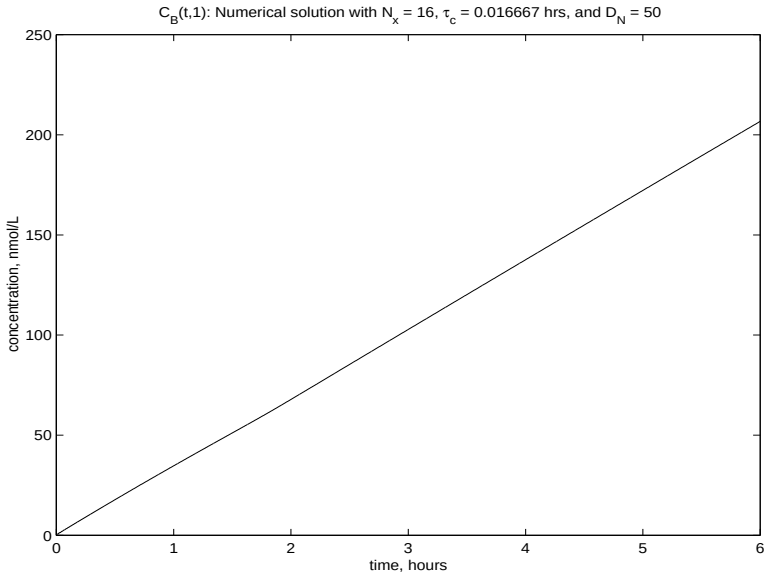

Figure 4: Concentration of dioxin at the exit from the liver, $C_B(t, 1)$.

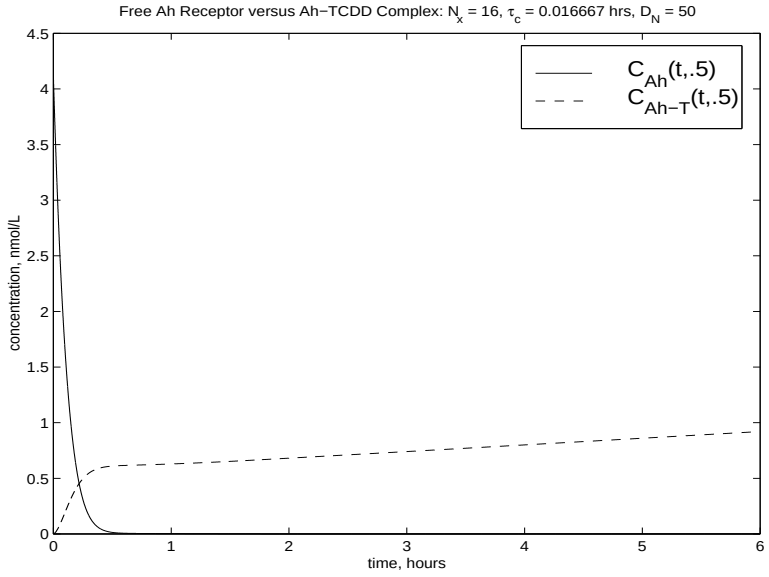

Figure 5: Concentrations of free Ah receptor protein and the bound Ah-TCDD complex. The Ah receptor becomes saturated after approximately thirty minutes.

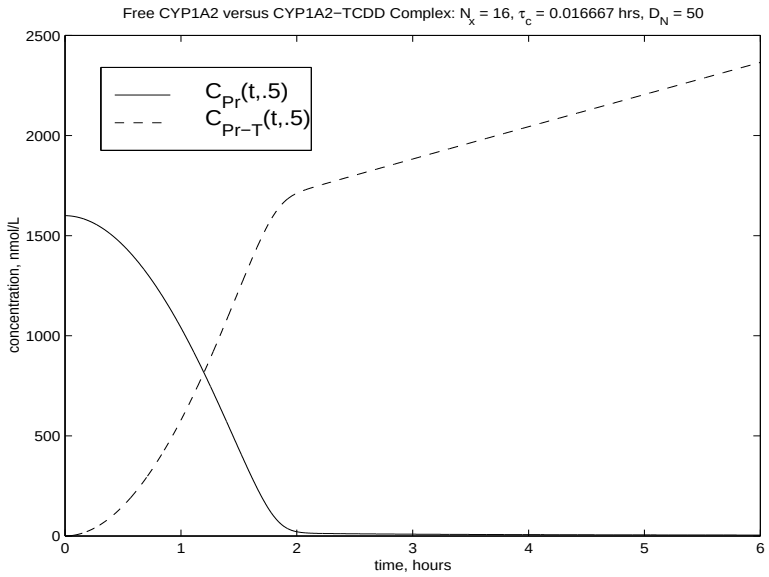

Figure 6: Concentrations of free CYP1A2 and the CYP1A2-TCDD complex. The protein becomes saturated after approximately two hours.

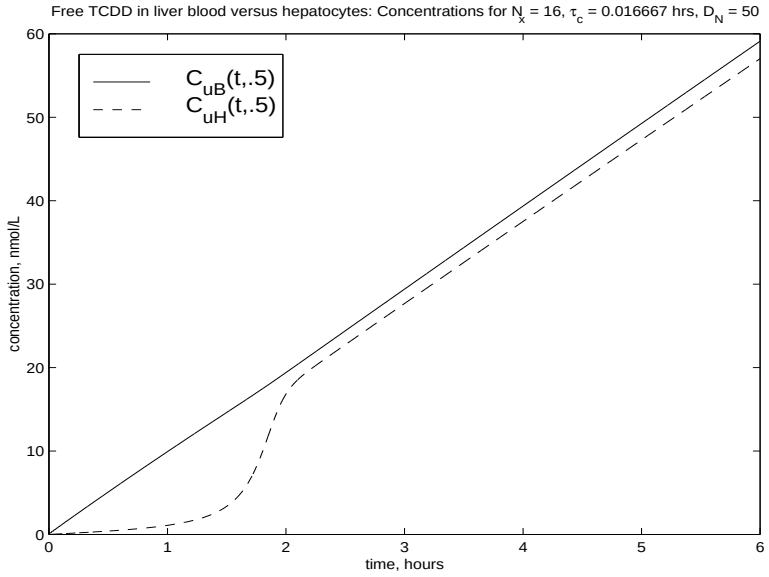

Figure 7: Concentrations of free TCDD in the liver blood (C_{u_B}) and hepatocytes (C_{u_H}) over a six hour period.

If we assume a constant rate of uptake of TCDD from a subcutaneous depot over a finite time interval $[0, T_{in}]$,

$$I(t) = \begin{cases} C_{in}, & t \leq T_{in} \\ 0, & t > T_{in}, \end{cases}$$

Eqn. (7) can be rewritten

$$\frac{dC_a(t)}{dt} = c_1 C_B(t - \tau_c, 1) - \mu C_a(t) + C_{in}\chi_{[0,T_{in}]}(t), \tag{9}$$

where $c_1 = \frac{Q_a}{V_a}$, $\mu = c_1 + k_e$, and

$$\chi_{[a,b]}(t) = \begin{cases} 1, & t \in [a, b], \\ 0, & \text{otherwise.} \end{cases}$$

We consider the only two possibilities of interest, $\tau_c = 0$ and $\tau_c > 0$.

Ignoring the Circulatory Delay

For the case $\tau_c = 0$, the analytic solution to (9) is

$$C_a(t) = \begin{cases} \frac{C_{in}}{\mu}(1 - e^{-\mu t}) + c_1 \int_0^t e^{-\mu(t-s)} C_B(s, 1) ds, & 0 \leq t \leq T_{in} \\ \frac{C_{in}}{\mu}(1 - e^{-\mu T_{in}}) + c_1 \int_0^t e^{-\mu(t-s)} C_B(s, 1) ds, & t \geq T_{in}. \end{cases} \tag{10}$$

From (10), it is clear that for any $t > 0$, the concentration of TCDD at the exit from the liver, $C_B(t, 1)$, contributes immediately to the predicted arterial blood concentration $C_a(t)$.

4.3.1 Predicted Solution with Circulatory Delay

We now consider the case $\tau_c > 0$. Let $t \in [0, T]$, with $T \ll T_{in}$. We assume a zero background concentration of TCDD in the system; in particular, $C_B(t, 1) = 0$ on $[-\tau_c, 0]$. On the initial interval of integration $[0, \tau_c]$, the rate of change of C_a is given by

$$\begin{gathered} \frac{dC_a}{dt}(t) = -\mu C_a(t) + C_{in}\chi_{[0,T_{in})}(t), \\ C_a(0) = 0. \end{gathered}$$

The analytic solution is

$$C_a(t) = \frac{C_{in}}{\mu}(1 - e^{-\mu t}), \quad t \in [0, \tau_c].$$

On the next interval of integration $[\tau_c, 2\tau_c]$, the governing differential equation for C_a is given by (9) with the initial condition

$$C_a(\tau_c) = \frac{C_{in}}{\mu}(1 - e^{-\mu \tau_c}).$$

The solution, for $t \in [\tau_c, 2\tau_c]$, is

$$\begin{aligned} C_a(t) &= e^{-\mu(t-\tau_c)} C_a(\tau_c) + \frac{C_{in}}{\mu}(1 - e^{-\mu(t-\tau_c)}) \\ &\quad + c_1 \int_{\tau_c}^t e^{-\mu(t-s)} C_B(s - \tau_c, 1) ds \\ &= e^{-\mu(t-\tau_c)} C_a(\tau_c) + C_a(t - \tau_c) + c_1 \int_{\tau_c}^t e^{-\mu(t-s)} C_B(s - \tau_c, 1) ds. \end{aligned}$$

The contribution to C_a from the liver, $C_B(t, 1)$, does not appear until $t > \tau_c > 0$. As shown in Figure 8, the concentration-time profile of the combined arterial/venous blood compartment illustrates this phenomenon and its impact on the solution over a period of ten delay intervals. The solution follows an apparent exponential curve on $[0, \tau_c]$; after this time, a marked increase in concentration is seen as the initial input of dioxin to the liver (that which has not been taken up by the hepatocytes) finally exits the organ and returns to the general circulation. As time progresses this sharp demarcation in solutions at the end of each delay interval diminishes.

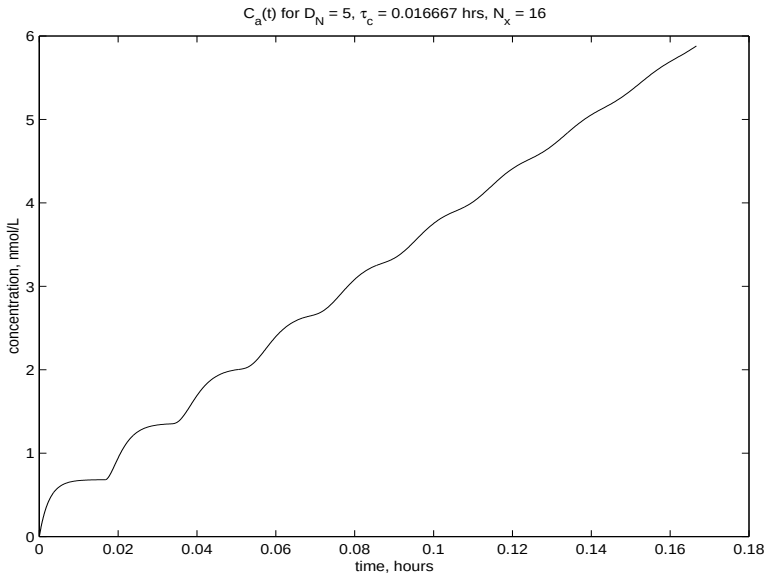

Figure 8: Predicted concentrations of TCDD in the combined arterial/venous blood supply, C_a, for a period of ten circulatory delay intervals.

4.3.2 Predictions of the Model with and without Circulatory Delay

The concentration of TCDD in the arterial/venous blood supply (C_a) is illustrated in Figure 9 for different values of τ_c ($0 \leq \tau_c \leq 1$ minute). Higher concentrations of TCDD are predicted for smaller values of τ_c due to the decrease in the length of time before input of TCDD from the liver compartment appears at the site of measurement in the venous blood. This would suggest that models which ignore the circulatory delay may result in an over-prediction of TCDD concentration. The predicted concentration of TCDD in the blood at the exit from the liver, $C_B(t, 1)$, is shown in Figure 10.

4.3.3 Dependence on the Axial Dispersion Number

In Section 4.3, we explained that the magnitude of the axial dispersion number does not affect the arterial/venous blood concentration, C_a, on the initial delay interval $[0, \tau_c]$. On $[\tau_c, 2\tau_c]$, however, we begin to see the effects of liver concentrations on the amount of TCDD in the arterial/venous blood supply. For $\mathcal{D}_N$ very small ($\mathcal{D}_N \to 0$), the model is driven predominantly by convective forces; that is, the predictions are closely related to that of a plug-flow model. As $\mathcal{D}_N$ increases ($\mathcal{D}_N \to \infty$), the model approaches one with a well-mixed state, with uniform concentrations along the length of the cylinder, so that input to the cylinder at $x = 0$ is immediately distributed along its length. This results in higher TCDD concentrations along the cylinder as compared to those predicted with lower values of $\mathcal{D}_N$. Figures 11 and 12 depict the variations in predicted concentrations for C_B as a function of x, after one minute and one hour, respectively. The effects of these variations on the arterial blood compartment are shown in Figure 13, as D_N varies from 5 to 1000.

4.3.4 Remarks on the Magnitude of the Dispersion Number

Roberts and Rowlands estimated the dispersion number to be between 0.1 and 0.2 for red blood cells and other non-eliminated solutes following a bolus input [12] and 0.2–0.5 at steady state following a constant input concentration [19]. They noted, however, that it is likely that dispersion numbers obtained for extracted solutes will generally be higher than those for substances that are not eliminated [12]. Moreover, binding of solutes to cellular constituents results in longer

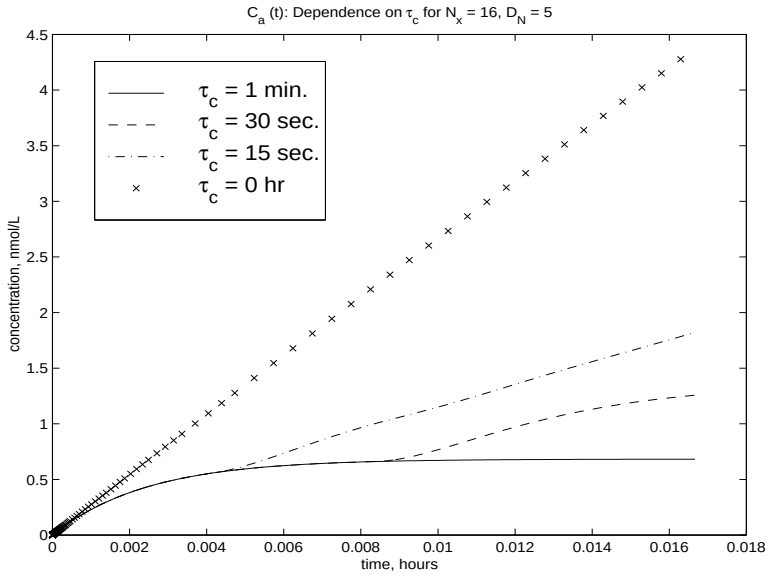

Figure 9: Predicted concentrations of TCDD in the combined arterial/venous blood supply as a function of the delay period, τ_c, for $0 \leq t \leq 1$ minute.

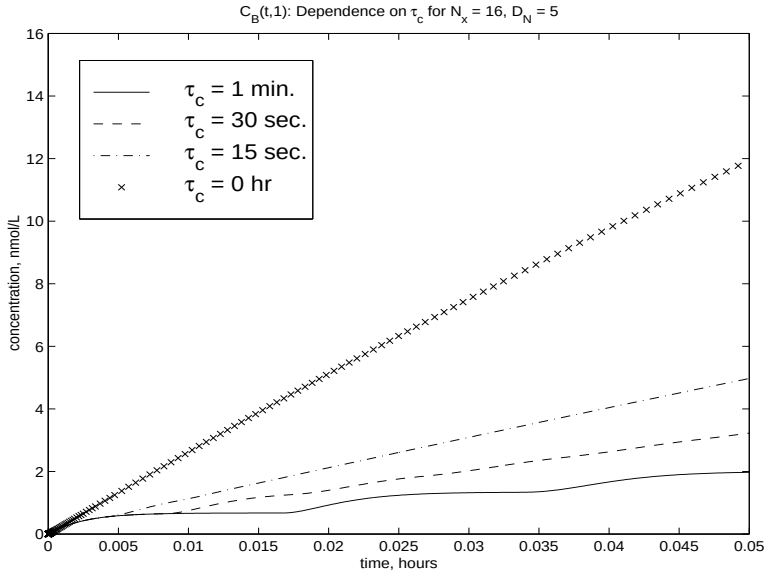

Figure 10: Predicted concentrations in blood at the exit from the liver as a function of the delay period, τ_c, for $0 \leq t \leq 3$ minutes.

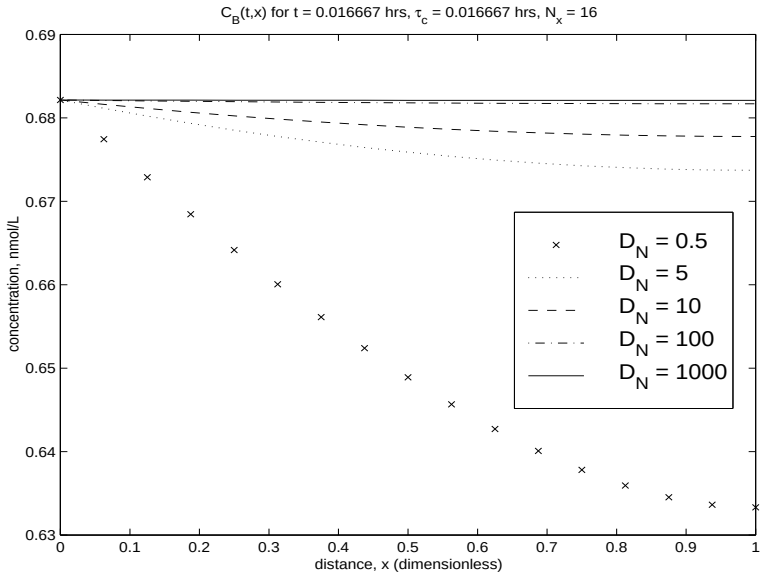

Figure 11: Predicted concentrations of TCDD in the liver blood compartment as a function of distance, x, and the axial dispersion number, $\mathcal{D}_N$, at time $t = 1$ minute.

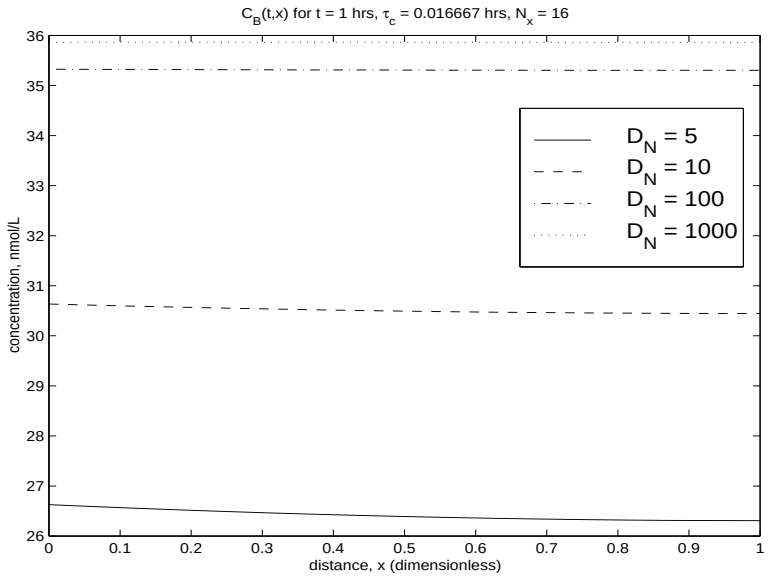

Figure 12: Predicted concentrations of TCDD in the liver blood compartment as a function of distance, x, and the axial dispersion number, $\mathcal{D}_N$, at time $t = 1$ hour.

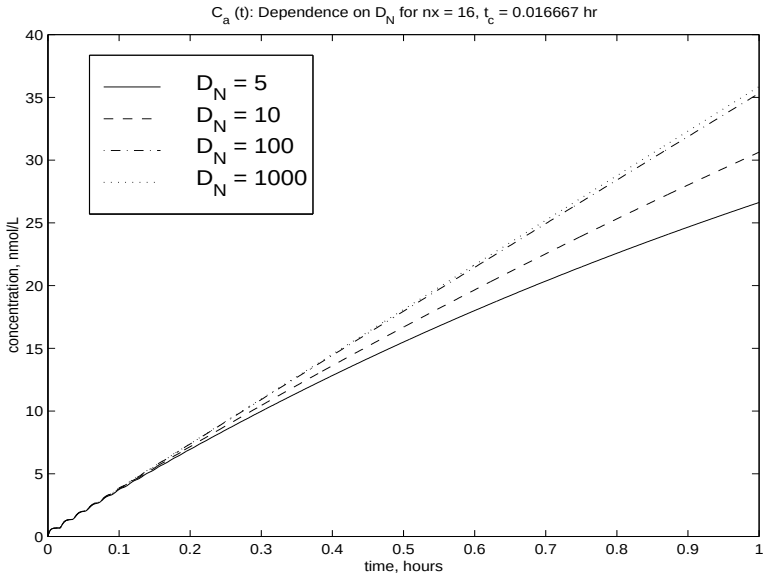

Figure 13: Predicted concentrations of TCDD in the combined arterial/venous blood compartment as a function of the axial dispersion number, $\mathcal{D}_N$.

residence times in the liver; solutes that are highly bound in the cells are retained in the liver for long periods of time while those that are confined to the sinusoidal bed pass through the liver quickly [12].

The dispersion number is dependent on blood flow rates, protein binding, elimination and hepatic cell permeability, and is probably also species-dependent [12]. In our investigations of the qualitative behavior of the TCDD model, we have used dispersion numbers varying from 0.5 to 1000. In simulations where the dispersion number was fixed and other parameters (such as the circulatory delay, τ_c) were varied, we chose to use values of $\mathcal{D}_N$ at least an order of magnitude higher than Roberts and Rowlands's estimate due to the likelihood that their estimates are too low for our model. TCDD is highly lipophilic [20] and enters the cells easily, where it binds to two intracellular proteins, the Ah receptor and CYP1A2. The dispersion model used in the data analysis of Roberts and Rowlands assumed first-order binding to cellular constituents. The more complex nonlinear chemical kinetics in our model may arguably correspond to a higher dispersion number. In addition, the majority of the parameters taken from the literature (e.g., [2, 5, 21, 22]) were estimated by fitting well-stirred models to experimental data. Therefore, although our investigations here were of a qualitative nature, the use of a high dispersion number may be quantitatively more in keeping with those parameter estimates. The magnitude of the dispersion number for the TCDD model is a question that is most properly addressed in the context of a parameter identification problem, which would involve fitting the model to experimental data.

5 Future Directions

In this presentation we studied the qualitative behavior of the TCDD model and its dependence on two parameters, the axial dispersion number, $\mathcal{D}_N$, and a circulatory delay, τ_c. We found that predicted concentrations of TCDD in the liver increased with either increasing dispersion number or decreasing circulatory delay. Furthermore, the model predicts spatial variations in cellular concentrations of dioxin at low dispersion numbers, a feature that the most commonly used model, the well-mixed model, does not provide.

Further analysis of the qualitative behavior of the system, including the effect of the induction delay, is currently underway. The model will be adapted for spatially-varying basal synthesis and induction of CYP1A2, thereby permitting comparisons to the multi-compartment liver model of

Andersen *et al.* [6]. The development of these types of advanced, spatially-dependent pharmacokinetic and pharmacodynamic models may play an important role in the development of risk assessment protocols for dioxin and other environmental toxins.

Acknowledgments

The authors thank Dr. Richard Albanese of the Mathematical Products Division, Air Force Research Laboratory (Brooks Air Force Base), for his generous encouragement and many productive discussions throughout the course of these investigations.

Nomenclature

Abbr.	Description	Units
$Aq_2(t)$	exit boundary condition term resulting from flux balance	$nmol/hr$
C_a	total arterial and venous blood TCDD concentration	$nmol/L$
C_{Ah}	concentration of available Ah receptor protein in hepatocytes	$nmol/L$
C_{Ah-T}	concentration of Ah receptor-TCDD complex in hepatocytes	$nmol/L$
C_B	total concentration of TCDD in liver blood	$nmol/L$
C_{Pr}	concentration of available CYP1A2 in hepatocytes	$nmol/L$
C_{Pr-T}	concentration of CYP1A2-TCDD complex in hepatocytes	$nmol/L$
C_{u_B}	concentration of unbound TCDD in liver blood	$nmol/L$
C_{u_H}	concentration of unbound TCDD in hepatocytes	$nmol/L$
$\mathcal{D}_N$	axial dispersion number	
f_{u_B}	fraction of TCDD unbound in the blood	
f_{u_D}	fraction of TCDD unbound in space of Disse	
$I(t)$	input concentration of TCDD at time t	$nmol/L/hr$
I_{Pr}	maximum rate of synthesis of CYP1A2 in the presence of TCDD	$nmol/L/hr$
k_{+1}	association rate constant of TCDD and Ah receptor	$L/nmol/hr$
k_{+2}	association rate constant of TCDD and CYP1A2	$L/nmol/hr$
k_{-1}	dissociation rate constant of Ah receptor-TCDD complex	$/hr$
k_{-2}	dissociation rate constant of CYP1A2-TCDD complex	$/hr$
k_3	apparent first-order metabolic clearance rate of TCDD	$/hr$
$k_{d(Ah)}$	rate constant for thermal inactivation of Ah receptor protein	$/hr$
$k_{d(Pr)}$	rate constant for degradation of CYP1A2	$/hr$
k_e	rest of body elimination term	$/hr$
$k_{s(Ah)}$	rate constant for synthesis of Ah receptor protein	$nmol/L/hr$
$k_{s(Pr)}$	rate constant for basal synthesis of CYP1A2	$nmol/L/hr$
P	permeability coefficient of the hepatocytes to TCDD	L/hr
Q	volumetric flow rate of liver blood	L/hr
Q_a	volumetric flow rate of venous blood	L/hr
τ_c	circulation delay	hr
τ_r	lag time between TCDD binding to Ah receptor and cellular response of CYP1A2 induction	hr
V_a	combined arterial and venous blood volumes	L
V_B	liver blood volume	L
V_D	Disse space volume	L
V_H	hepatocyte volume	L
x	dimensionless spatial variable ($x = 0$ corresponds to the inlet, $x = 1$ to the outlet)	

References

[1] H. T. Banks, C. J. Musante, and H. T. Tran. A dispersion model for the hepatic uptake and elimination of 2,3,7,8-tetrachlorodibenzo-*p*-dioxin. *CRSC-TR97-29, North Carolina State University, September, 1997; Mathematical and Computer Modelling*, 28(1):9–29, 1998.

[2] H.-W. Leung, D. J. Paustenbach, F. J. Murray, and M. E. Andersen. A physiological pharmacokinetic description of the tissue distribution and enzyme-inducing properties of 2,3,7,8-tetrachlorodibenzo-*p*-dioxin in the rat. *Toxicology and Applied Pharmacology*, 103:399–410, 1990.

[3] H.-W. Leung, R. H. Ku, D. J. Paustenbach, and M. E. Andersen. A physiologically based pharmacokinetic model for 2,3,7,8-tetrachlorodibenzo-*p*-dioxin in C57BL/6J and DBA/2J mice. *Toxicology Letters*, 42:15–28, 1988.

[4] W. L. Roth, S. Ernst, L. W. D. Weber, L. Kerecsen, and K. K. Rozman. A pharmacodynamically responsive model of 2,3,7,8-tetrachlorodibenzo-*p*-dioxin (TCDD) transfer between liver and fat at low and high doses. *Toxicology and Applied Pharmacology*, 127:151–162, 1994.

[5] M. E. Andersen, J. J. Mills, M. L. Gargas, L. Kedderis, L. S. Birnbaum, D. Neubert, and W. F. Greenlee. Modeling receptor-mediated processes with dioxin: Implications for pharmacokinetics and risk assessment. *Risk Analysis*, 13(1):25–36, 1993.

[6] M. E. Andersen, L. S. Birnbaum, H. A. Barton, and C. R. Ecklund. Regional hepatic CYP1A1 and CYP1A2 induction with 2,3,7,8-tetrachlorodibenzo-*p*-dioxin evaluated with a multicompartment geometric model of hepatic zonation. *Toxicology and Applied Pharmacology*, 144:145–155, 1997.

[7] M. E. Andersen, C. R. Ecklund, J. J. Mills, H. A. Barton, and L. S. Birnbaum. A multicompartment geometric model of the liver in relation to regional induction of cytochrome P450s. *Toxicology and Applied Pharmacology*, 144:135–144, 1997.

[8] A. Poland and E. Glover. Stereospecific, high affinity binding of 2,3,7,8-tetrachlorodibenzo-*p*-dioxin by hepatic cytosol. *Journal of Biological Chemistry*, 251(16):4936–4946, 1976.

[9] A. Poland, P. Teitelbaum, and E. Glover. [^{125}I]2-Iodo-3,7,8-trichlorodibenzo-*p*-dioxin-binding species in mouse liver induced by agonists for the Ah receptor: Characterization and identification. *Molecular Pharmacology*, 36:113–120, 1989.

[10] R. Voorman and S. D. Aust. Specific binding of polyhalogenated aromatic hydrocarbon inducers of cytochrome P-450d to the cytochrome and inhibition of its estradiol-2-hydroxylase activity. *Toxicology and Applied Pharmacology*, 90:69–78, 1987.

[11] C. J. Musante. *A Distributed Parameter Model for Spatially Dependent Hepatic Processing of 2,3,7,8-Tetrachlorodibenzo-p-dioxin*. PhD thesis, North Carolina State University, Raleigh, NC, August 1998.

[12] M. S. Roberts and M. Rowland. A dispersion model of hepatic elimination: 1. Formulation of the model and bolus considerations. *Journal of Pharmacokinetics and Biopharmaceutics*, 14(3):227–260, 1986.

[13] H. T. Banks and C. J. Musante. Well-posedness for a class of abstract nonlinear parabolic systems with time delay. *CRSC-TR97-30, North Carolina State University, September 1997; Nonlinear Analysis: Theory, Methods, and Applications*, 35:629–648.

[14] H. T. Banks, C. J. Musante, and J. K. Raye. Parameter estimation for a class of abstract nonlinear parabolic systems. *JOURNAL NAME*, submitted.

[15] H. T. Banks, D. S. Gilliam, and V. L. Shubov. Global solvability for damped abstract nonlinear hyperbolic systems. *Differential and Integral Equations*, 10:309–332, 1997.

[16] H. T. Banks, R. C. Smith, and Y. Wang. *Smart Material Structures: Modeling Estimation, and Control.* Masson/J. Wiley & Sons.

[17] R. Bellman and K. L. Cooke. *Differential-Difference Equations.* Rand Corporation, 1963.

[18] L. F. Shampine and M. W. Reichelt. The MATLAB ODE Suite. *SIAM Journal on Scientific Computing*, 18(1):1–22, 1997.

[19] M. S. Roberts and M. Rowland. A dispersion model of hepatic elimination: 2. Steady-state considerations–influence of hepatic blood flow, binding within blood, and hepatocellular enzyme activity. *Journal of Pharmacokinetics and Biopharmaceutics*, 14(3):261–288, 1986.

[20] S.A. Skene, I.C. Dewhurst, and M. Greenberg. Polychlorinated dibenzo-*p*-dioxins and polychlorinated dibenzofurans: The risks to human health, A review. *Human Toxicology*, 8:173–203, 1989.

[21] X. Wang, M. J. Santostefano, M. V. Evans, V. M. Richardson, J. J. Diliberto, and L. S. Birnbaum. Determination of parameters responsible for pharmacokinetic behavior of TCDD in female Sprague-Dawley rats. *Toxicology and Applied Pharmacology*, 147:151–168, 1997.

[22] M. C. Kohn, G. W. Lucier, G. C. Clark, C. Sewall, A. M. Tritscher, and C. Portier. A mechanistic model of effects of dioxin on gene expression in the rat liver. *Toxicology and Applied Pharmacology*, 120:138–154, 1993.